Rising Bubbles

MCEN 5151 Flow Visualization - Team Third Report

Luke Freyhof

November 21, 2025

Special thanks to Xeen Meighan and Alana Martinez who helped with the imaging process.

Statement of Meaning Figure 1 was created for the third team flow visualization assignment and shows bubbles rising in a rectangular container filled with a glycerin-water mixture. The bubbles were created by forcing air out of a plastic pipette tip, which was positioned immediately below the imaging frame. Glycerin is more viscous than water, which ultimately causes bubbles in glycerin to rise more slowly than bubbles in water, as visualized in the video I created. Bubble size also affects rise speed: smaller bubbles rise more slowly than larger bubbles. To add color to the imaging setup (for artistic purposes), I used blue dye to color the glycerin-water mixture and a few drops of purple dye to create the bubble trails. The Morton and Bond numbers can be used to describe the shape and behavior of a rising bubble. The bubble speed is compared to the predicted speed of a bubble given the flow conditions.

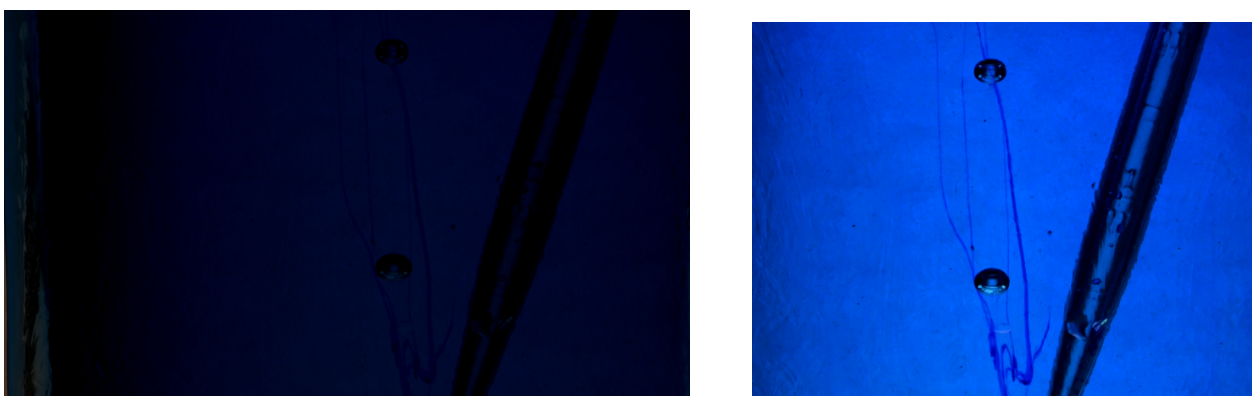

(A) Frame extracted from unedited video

(B) Frame extracted from edited video

Figure 1: Bubbles rising through a glycerin-water mixture.

Setup and Flow Description This flow was created using a small rectangular vase, a pipette, glycerin, water, and food coloring. 175 mL of glycerin was mixed with 50 mL of water to form the mixture; multiple drops of blue food coloring were added to dye the mixture. A 10 W, 4500 K color temperature LED panel lamp with a white paper light-diffusing sheet served as a backlight behind the vase. To create the rising bubbles, 1 mL of densely dyed (purple) glycerin from a separate container was captured with the pipette and released near the bottom of the rectangular vase. After the purple dyed glycerin was released, the pipette was compressed further, ejecting bubbles

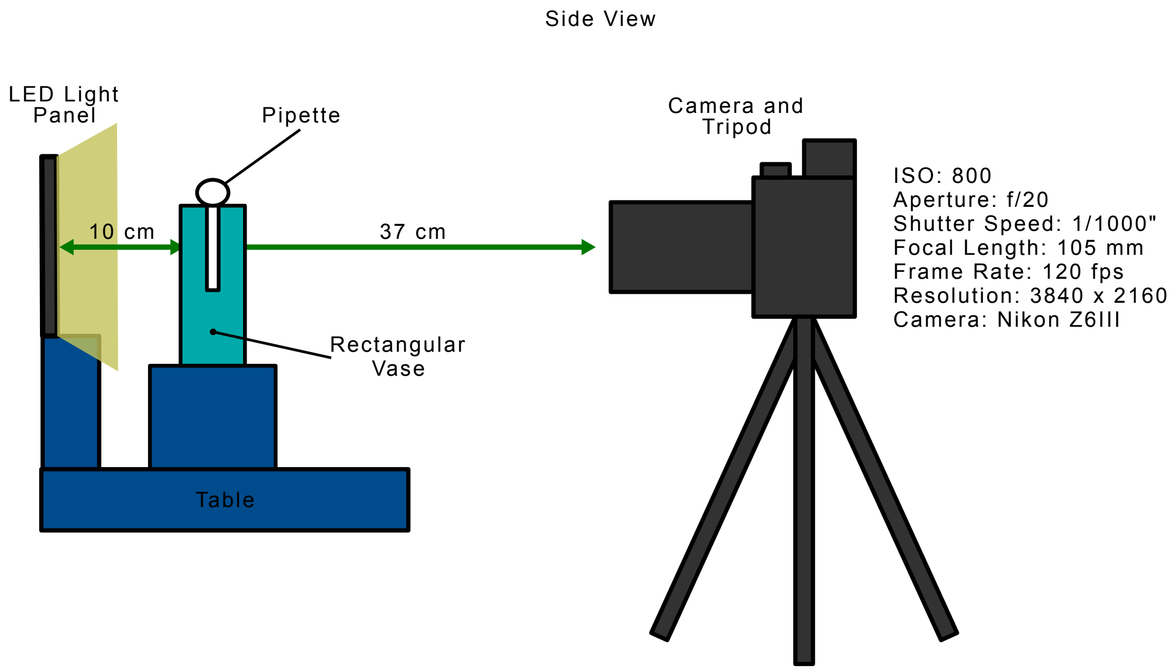

Figure 2: Side view of visualization setup

that traveled upward through the purple glycerin mixture. A 120 frame per second video was recorded of the rising bubbles and analyzed to calculate the bubble characteristics and speeds.

A Nikon Z6III camera with a 105 mm f/2.8 Nikkor macro lens recorded the videos from 37 cm away, as shown in Figure 2. The macro lens and camera distance were chosen to capture the details of the rising bubbles with a high spatial resolution. To ensure the camera remained stationary while recording, a tripod was used. The video of the rising bubbles was recorded at 120 frames per second with a resolution of 3840×2160 pixels, ensuring that the quick bubble movements and details were captured.

When bubbles rise through an ambient fluid, they do so because of buoyant forces. Air is less dense than water (and glycerin), which means that the gravitational forces acting on the bubble are smaller than a those acting on an identical volume of ambient fluid (glycerin-water mixture). However, the hydrostatic pressure forces acting on both of these identical volumes are identical. Because the pressure forces acting on the bubble volume are higher on the bottom of the bubble in comparison to the top of the bubble, there is a net upward pressure force. This net upward pressure force is larger than the gravitational force acting on the air in the bubble, resulting in a total net upward force on the bubble. When a total net force is applied to an object, it will begin to accelerate (think about Newton's second law, $F = ma$). In the case of the bubble, the net acceleration is upward, which is why bubbles rise.

The buoyant force isn't the only force that acts on the bubble — when the bubble rises, a drag force slows it down. This drag force increases as the bubble velocity increases, eventually reaching an equilibrium point where it is equivalent to the upward buoyancy force. When this occurs, the bubble stops accelerating and continues traveling upward at its terminal velocity. The terminal velocity for a rising bubble can be estimated using models fitted to experimental data.

Dimensionless numbers, such as the Morton and Bond numbers, can be used to describe and compare bubbles rising through different ambient media. The Bond number describes the relative scales of surface tension and gravitational forces, while the Morton number is used to help describe the shapes of bubbles. If the Bond number is very small, the gravitational and buoyancy forces on a bubble will dominate the surface tension forces, leading the bubble to deform from spherical shape. Conversely, if the Bond number is large, the gravitational and buoyancy forces will cause the bubble to deform from its spherical shape. Because the Bond number scales with the square of the bubble size (see Equation 1), larger bubbles are more likely than small bubbles to deform from a spherical shape.[1] Similarly, the Morton number (see Equation 2) describes bubble shape by relating gravitational, viscous, and surface tension forces in a fluid.[1] If the surface tension forces are high compared to the viscous and gravitational/buoyancy forces, then the bubble will remain spherical. If the surface tension forces are low compared to the other forces, the bubble will take on an ellipsoidal or irregular shape.

Constant	Description	Value
μ	viscosity of glycerin-water mixture	6.4099×10^{-2} Ns/m^2[2]
μ_w	viscosity of water	9.532×10^{-4} Ns/m^2[3]
ρ	density of glycerin-water mixture	1.2019×10^3 kg/m^3[2]
ρ_{air}	density of air	1.196 kg/m^3[4]
$\Delta\rho$	difference between air and mixture density	1.201×10^3 kg/m^3
U_T	bubble terminal velocity	$0.2\,\mathrm{m\,s^{-1}}$ (measured)
d_e	large ellipsoidal diameter of bubble	3.953×10^{-3} m
σ	surface tension constant	$6.74 \times 10^{-2}\,\mathrm{N\,m^{-1}}$
g	gravitational acceleration	9.81 m/s^2
J, H, N_D	bubble model constants	varies
Re	Reynolds number	varies

Table 1: Constants and measurements. Some measurements (terminal velocity) were acquired using Fiji.[5]

$$\mathrm{Bo} = \frac{g\Delta\rho d_e^2}{\sigma} = \frac{(9.81)(1200.7)(3.953 \times 10^{-3})^2}{(6.74 \times 10^{-2})} = 2.73 \tag{1}$$

$$\mathrm{Mo} = \frac{g\mu^4\Delta\rho}{\rho^2\sigma^3} = \frac{(9.81)(6.4099 \times 10^{-2})^4(1200.7)}{(1201.9)^2(6.74 \times 10^{-2})^3} = 4.57 \times 10^{-4} \tag{2}$$

$$H = \frac{4}{3}EoMo^{-0.149}(\frac{\mu}{\mu_w})^{-0.14} = \frac{4}{3}(2.73)(4.57 \times 10^{-4})^{-0.149}(\frac{6.4099 \times 10^{-2}}{9.532 \times 10^{-2}})^{-0.14} = 6.35 \tag{3}$$

$$J = 0.94H^{0.757} = 0.94(6.35)^{0.757} = 3.81 \tag{4}$$

$$U_T = \frac{\mu}{\rho d_e}Mo^{-0.149}(J - 0.857) \tag{5}$$

$$= \frac{6.4099 \times 10^{-2}}{(1.2019 \times 10^3)(3.953 \times 10^{-3})}(4.57 \times 10^{-4})^{-0.149}(3.81 - 0.857) = 125.36\,\mathrm{mm\,s^{-1}} \tag{6}$$

The predicted terminal velocity of the bubble (shown in Equation 5) was less than the actual measured terminal velocity (see Table 1). The equations used to predict the bubble velocity were from Zheng *et al.*.[1] This discrepancy between predicted and measured velocity could have been caused by the poor choice of some of the contants, which were estimated from tables rather than measured directly.

Visualization Technique As described previously, bubbles were released from a pipette into a glycerin-water mixture. The ambient mixture was dyed. Additional dye was placed near the bubble release point, giving the bubbles dye trails as they rose through the ambient mixture. A 10 W LED light panel was placed behind the rectangular vase with the glycerin-water mixture to illuminate the rising bubbles.

Photographic Technique 29 cm is the minimum focus distance of the Nikkor 105 mm f/2.8 macro lens that was used to record the videos.[6] As shown in Figure 2, a Nikon Z6III with an f/20 aperture, a 1/1000 second shutter speed, and a 755 ISO setting were used to capture the image. The Z6III digitally recorded videos at 120 fps with dimensions of 3840×2160 pixels and a view angle of $23.167 \times 15.333°$.[6]

After cropping and editing, the final video was played back at 15 fps. Exposure was increased in the video editing software to better visualize the bubbles, which were rather dark after being recorded with too little exposure. The video playback was slowed down to allow the viewer to see the rising bubbles. Video compilation was done with KdenLive.

Analysis and Reflection As mentioned previously, the video was underexposed. I didn't have a good reason for recording the video with an aperture of f/20. That was simply a leftover camera setting from a previous video recording, and I was too negligent to change it. Still, the flow physics are shown well thanks to the dynamic range of the camera — I was able to increase the exposure in post processing with little to no side effects. In the future, I would have also considered shortening my shutter speed, because the motion blur I calculated was 76 pixels per frame or 1.699 mm. The spatial resolution of the photo was suitable at 0.022 mmperpixel. I could have also improved the framing of the video by recording the setup in portrait mode, including the end of the pipette tip in the frame.

References

[1] L. Zheng and P. D. Yapa, “Buoyant Velocity of Spherical and Nonspherical Bubbles/Droplets,” *Journal of Hydraulic Engineering*, vol. 126, no. 11, pp. 852–854, Nov. 1, 2000, ISSN: 0733-9429. DOI: 10.1061/(ASCE)0733-9429(2000)126:11(852). [Online]. Available: https://ascelibrary.org/doi/10.1061/%28ASCE%290733-9429%282000%29126%3A11%28852%29 (visited on 11/19/2025).

[2] “Calculate density and viscosity of glycerol/water mixtures.” (), [Online]. Available: https://www.met.reading.ac.uk/~sws04cdw/viscosity_calc.html (visited on 11/19/2025).

[3] “Water - Dynamic and Kinematic Viscosity at Various Temperatures and Pressures.” (), [Online]. Available: https://www.engineeringtoolbox.com/water-dynamic-kinematic-viscosity-d_596.html (visited on 11/19/2025).

[4] “Air Viscosity: Dynamic and Kinematic Viscosity at Various Temperatures and Pressures.” (), [Online]. Available: https://www.engineeringtoolbox.com/air-absolute-kinematic-viscosity-d_601.html (visited on 11/03/2025).

[5] J. Schindelin, I. Arganda-Carreras, E. Frise, *et al.*, “Fiji: An open-source platform for biological-image analysis,” *Nature Methods*, vol. 9, no. 7, pp. 676–682, Jul. 2012, ISSN: 1548-7105. DOI: 10.1038/nmeth.2019. [Online]. Available: https://www.nature.com/articles/nmeth.2019 (visited on 09/24/2025).

[6] “Nikon Z 105mm f/2.8 MC Macro Review.” (), [Online]. Available: https://www.kenrockwell.com/nikon/z/105mm-f28.htm (visited on 11/04/2025).